

## Wetting state on hydrophilic and hydrophobic micro-textured surfaces: Thermodynamic analysis and X-ray visualization

Dong In Yu, Seung Woo Doh, Ho Jae Kwak, Hie Chan Kang, Ho Seon Ahn, Hyun Sun Park, Moriyama Kiyofumi, and Moo Hwan Kim

Citation: [Applied Physics Letters](#) **106**, 171602 (2015); doi: 10.1063/1.4919136

View online: <http://dx.doi.org/10.1063/1.4919136>

View Table of Contents: <http://scitation.aip.org/content/aip/journal/apl/106/17?ver=pdfcov>

Published by the [AIP Publishing](#)

---

### Articles you may be interested in

[Does surface roughness amplify wetting?](#)

J. Chem. Phys. **141**, 184703 (2014); 10.1063/1.4901128

[Wetting of soap bubbles on hydrophilic, hydrophobic, and superhydrophobic surfaces](#)

Appl. Phys. Lett. **102**, 254103 (2013); 10.1063/1.4812710

[Reversible switching between isotropic and anisotropic wetting by one-direction curvature tuning on flexible superhydrophobic surfaces](#)

Appl. Phys. Lett. **98**, 081902 (2011); 10.1063/1.3556585

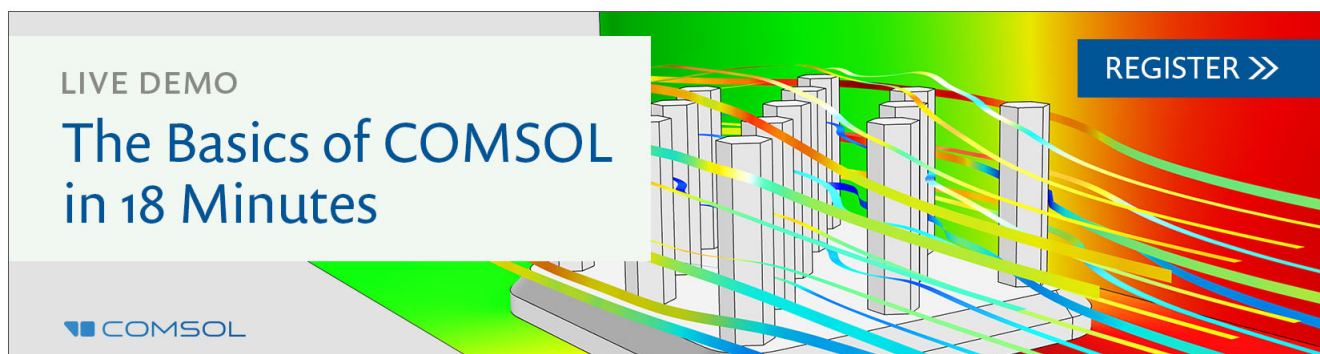
[Surface texture and wetting stability of polydimethylsiloxane coated with aluminum oxide at low temperature by atomic layer deposition](#)

J. Vac. Sci. Technol. A **28**, 1330 (2010); 10.1116/1.3488604

[Effect of self-affine fractal characteristics of surfaces on wetting](#)

Appl. Phys. Lett. **96**, 063112 (2010); 10.1063/1.3309690

---

A promotional banner for COMSOL software. On the left, a white box contains the text 'LIVE DEMO' and 'The Basics of COMSOL in 18 Minutes'. The COMSOL logo is at the bottom left. The background features a 3D model of a micro-textured surface with several vertical pillars, overlaid with colorful streamlines representing fluid flow. A blue button with white text 'REGISTER >>' is located in the top right corner.

LIVE DEMO

# The Basics of COMSOL in 18 Minutes

COMSOL

REGISTER >>

## Wetting state on hydrophilic and hydrophobic micro-textured surfaces: Thermodynamic analysis and X-ray visualization

Dong In Yu,<sup>1</sup> Seung Woo Doh,<sup>2</sup> Ho Jae Kwak,<sup>1</sup> Hie Chan Kang,<sup>3</sup> Ho Seon Ahn,<sup>4</sup> Hyun Sun Park,<sup>2,a)</sup> Moriyama Kiyofumi,<sup>2</sup> and Moo Hwan Kim<sup>1,2</sup>

<sup>1</sup>Department of Mechanical Engineering, POSTECH, Pohang 790-784, South Korea

<sup>2</sup>Division of Advanced Nuclear Engineering, POSTECH, Pohang 790-794, South Korea

<sup>3</sup>School of Mechanical and Automotive Engineering, Kunsan National University, Kunsan 573-701, South Korea

<sup>4</sup>Division of Mechanical System Engineering, Incheon National University, Incheon 406-772, South Korea

(Received 16 January 2015; accepted 16 April 2015; published online 29 April 2015)

In this study, the wetting state on hydrophobic and hydrophilic micro-textured surfaces was investigated. High spatial resolution synchrotron X-ray radiography was used to overcome the limitations in visualization in previous research and clearly visualize the wetting state for each droplet under quantified surface conditions. Based on thermodynamic characteristics, a theoretical model for wetting state depending on the chemical composition (intrinsic contact angle) and geometrical morphology (roughness ratio) of the surfaces was developed. © 2015 AIP Publishing LLC.

<http://dx.doi.org/10.1063/1.4919136>

Wetting is one of the key fundamental physical phenomena in liquid-solid contact systems that are widely encountered in nature and engineering applications. Recently, to improve surface wettability,<sup>1,2</sup> micro-electromechanical systems have been used to develop well-designed textured surfaces for application in various fields including self-cleaning,<sup>3,4</sup> water-proofing,<sup>5</sup> hydrodynamic friction reduction,<sup>6</sup> anti-biofouling,<sup>7-9</sup> and thermal and energy systems.<sup>10-12</sup>

Surface wettability is the ability of a liquid to maintain contact with a solid surface as a result of intermolecular interactions when the two are brought into contact. This ability is estimated based on the wetting state of a water droplet on the surface, and is generally quantified using the apparent contact angle,  $\theta_A$ . When a water droplet rests a textured surface, as shown in Fig. 1, various wetting states can be observed depending on the surface conditions. In previous reports, hydrophilic textured surfaces are fully wetted by water droplets.<sup>13</sup> In this case, if a droplet has a partial spherical shape, the wetting state of the droplet is defined as the Wenzel state.<sup>1</sup> However, if a droplet has a precursor (liquid film) that stretches out from the liquid drop along the surface, the wetting state is called the hemi-wicking state (“sunny-side-up” in other literature<sup>14</sup>). Hydrophobic textured surfaces are generally only partially wetted, i.e., the droplet is in the Cassie-Baxter state.<sup>15</sup> In some cases, droplets on hydrophobic textured surfaces have a Wenzel state or mixed state (where the Wenzel and Cassie states coexist).<sup>16</sup>

To estimate the apparent contact angle to quantify the surface wettability, the wetting state should be estimated. According to the previous wetting model,<sup>1,2,15,17</sup> the apparent contact angle is estimated on the basis of the chemical composition and geometric morphology of the surface. The chemical composition is a natural material characteristic of the solid surface and is quantified based on the intrinsic contact angle  $\theta_0$ , which is defined as the equilibrium contact

angle of a water droplet on the ideal smooth surface. The geometric morphology is a mechanical characteristic of the solid surface and is quantified in terms of the roughness ratio, defined as the ratio of the wetted area to the projected area.<sup>2</sup> On the textured surface with the same geometric morphology, since the wetted area is different depending on the wetting state, the roughness ratio is different depending on the wetting state. Therefore, the wetting state must be estimated to allow the apparent contact angle to be estimated.

Although wetting state has been extensively explored in previous reports,<sup>13,14,16,18-37</sup> the majority of these previous reports have focused on hydrophobic textured surfaces. Besides the wetting state was inferred from visible-wavelength images, making it difficult to identify the physical behavior at the vicinity of the micro-pillars on the test surfaces. Therefore, the precise visualization of wetting phenomena on micro-nanoscaled surfaces is crucial for understanding such wetting phenomena. From this perspective, we employed synchrotron X-ray radiography with high spatial resolution to overcome the challenges in visualization and used the results to develop a theoretical model for wetting state on hydrophobic and hydrophilic micro-textured surfaces. Micro-textured surfaces with well-defined

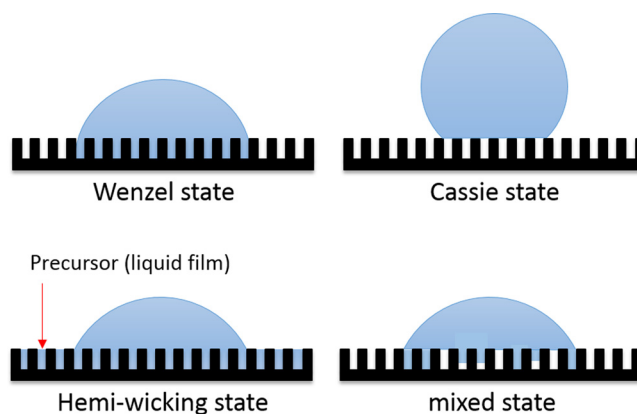


FIG. 1. Various wetting states.

<sup>a)</sup>Author to whom correspondence should be addressed. Electronic mail: [hejsunny@postech.ac.kr](mailto:hejsunny@postech.ac.kr)

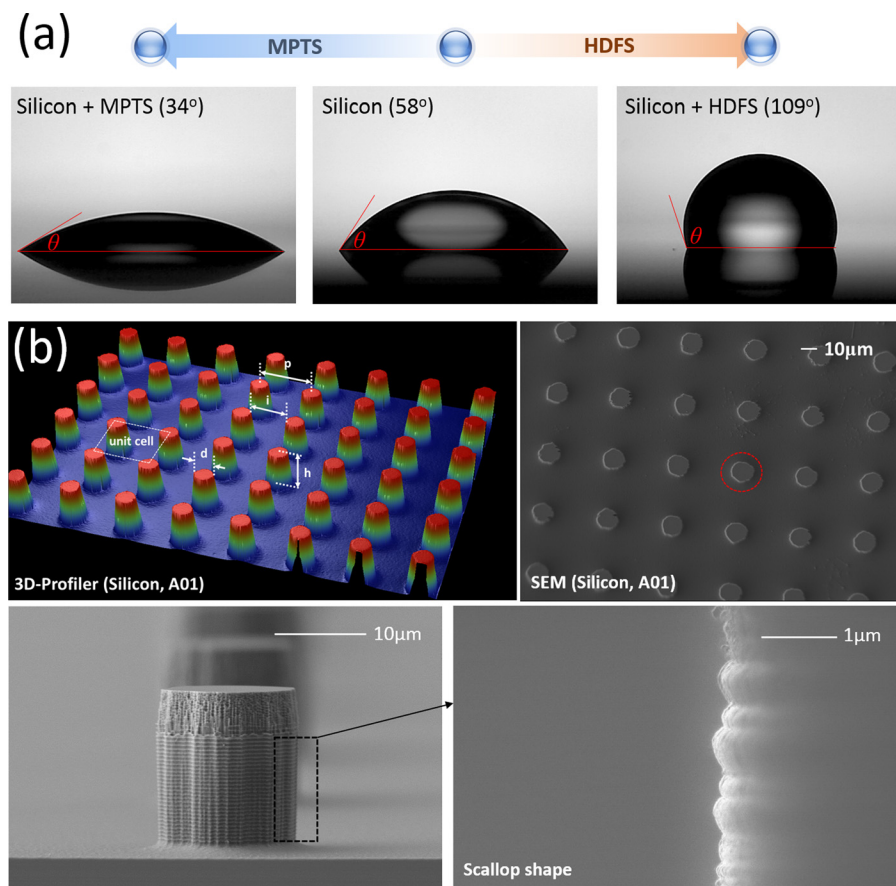


FIG. 2. (a) Static contact angles on surfaces with and without SAM coatings. A  $6.3 \mu\text{l}$  droplet of distilled ionized water was placed on the surface, and the static contact angle was measured by an automatic goniometer. The visible images were obtained using the microscope of the goniometer ( $8.69 \mu\text{m}/\text{pixel}$ ). (b) Images of test sections (3D-Profilometer, SEM).

surface conditions were fabricated to allow quantitative analysis of the wetting state. The wetting state was clearly defined for each droplet placed on the surface under quantified conditions on the basis of the images obtained from the synchrotron X-ray radiography. Based on thermodynamics, a theoretical model to define the wetting state depending on the surface conditions was developed.

Quantitative analysis of the wetting state required test sections with well-defined surface conditions. Therefore, the micro-textured surfaces coated with a self-assembled monolayer (SAM) were fabricated to produce surfaces with well-defined chemical compositions and geometric morphologies. To obtain different chemical surface compositions, the silicon surfaces were coated with hydrophilic (mercaptopropyl-trimethoxy-silane: MPTS) and hydrophobic (heptadecafluoro-1,1,2,2-tetrahydrodecyltrichlorosilane: HDFFS) SAMs. As shown in Fig. 2(a), the intrinsic contact angles of the silicon surface ( $\theta_0 = 58^\circ$ ) were  $34^\circ$  and  $109^\circ$  for the hydrophilic and hydrophobic SAM coatings, respectively. To obtain different geometric surface morphologies, textured surfaces with various micro-pillar arrays were fabricated using conventional lithography and dry-etching methods, as shown in Fig. 2(b). The dimensions of the micro-pillars on each fabricated surface were measured using a 3D-profiler and high-resolution field-emission scanning electron microscope (FE-SEM). According to the Wenzel state (W) and Cassie-Baxter state (C-B), the roughness ratio  $f$  was calculated in terms of the geometry and array of pillars (see the supplementary material for details<sup>38</sup>). In this study, micro-pillars with four different diameters (A:  $15 \mu\text{m}$ , B:  $45 \mu\text{m}$ , C:  $75 \mu\text{m}$ , and D:  $105 \mu\text{m}$ ) and three intervals between micro-pillars (“01:”  $25 \mu\text{m}$ , “02:”  $55 \mu\text{m}$ , and

“03:”  $85 \mu\text{m}$ ) were used to give 13 different surface morphologies (including the flat surface), as listed in Table I. These combinations were prepared with the three wetting cases (silicon surface, hydrophilic surface with MPTS SAM, and hydrophobic surface with HDFFS SAM) to obtain a total of 39 different test surfaces covering  $\theta_0 = 34^\circ, 58^\circ, \text{ and } 109^\circ$ ,  $1.0 < f_W < 2.0$  and  $0.02 < f_{C-B} < 1.0$ .

For visualization of the wetting states, synchrotron X-ray radiography with a spatial resolution of  $1.74 \mu\text{m}/\text{pixel}$  at the 6D beam-line of the Pohang Light Source-II (PLS-II) in Korea was used to visualize the micro-pillars on the

TABLE I. Geometric properties of the micro-textured surfaces.

No.	d ( $\mu\text{m}$ )	p ( $\mu\text{m}$ )	i ( $\mu\text{m}$ )	h ( $\mu\text{m}$ )	$f_W^a$	$f_{C-B}^a$
Flat	...	...	...	...	1	1
A01	16.13	40.02	23.89	20.06	2.00	0.13
A02	16.05	70.03	53.98	19.24	1.31	0.04
A03	14.73	100.50	85.77	19.90	1.14	0.02
B01	46.30	70.34	24.04	18.52	1.86	0.34
B02	47.62	100.01	52.39	17.95	1.42	0.18
B03	47.62	129.86	82.23	19.83	1.28	0.11
C01	76.68	99.85	23.18	21.54	1.82	0.46
C02	76.36	130.33	53.97	18.61	1.41	0.27
C03	76.36	159.86	83.50	18.34	1.27	0.18
D01	107.31	130.17	22.86	22.12	1.69	0.53
D02	106.20	159.86	53.66	21.84	1.45	0.35
D03	106.68	189.23	82.55	20.51	1.30	0.25

<sup>a</sup> $f_W$  and  $f_{C-B}$  are the roughness ratio for the Wenzel state and Cassie-Baxter state, respectively.



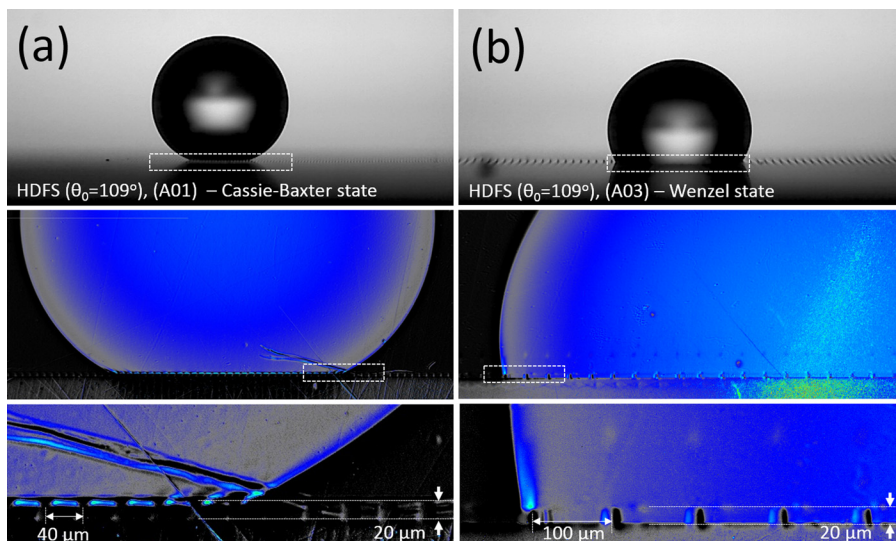


FIG. 3. Visualization of wetting state on micro-textured surfaces with HDFs coating using visible light and X-rays; (a) A01 ( $d = 15 \mu\text{m}$ ,  $p = 40 \mu\text{m}$ , and  $h = 20 \mu\text{m}$ ) and (b) A03 ( $d = 15 \mu\text{m}$ ,  $p = 100 \mu\text{m}$ , and  $h = 20 \mu\text{m}$ ). The lines across of the final image at Fig. 3(a) are caused by the local scratch at the scintillator screen.

micro-textured surfaces. A valuable advantage of this technique compared with photography is that it enabled us to clearly distinguish the interface between the silicon structure and water, because both materials have very different linear attenuation coefficients for X-rays. The detailed procedure used to visualize the wetting state with X-rays and information on PLS-II are described in the supplementary material.<sup>38</sup>

The dependence of wetting state on surface conditions was clearly visualized based on the obtained synchrotron X-ray radiography images. On the micro-textured surfaces with HDFs coating ( $\theta_0 = 109^\circ$ ), the Wenzel and Cassie-Baxter wetting states were observed depending on the geometric conditions of the surface. Surfaces with smaller intervals between the micro-pillars were only partially wetted, as shown in Fig. 3(a), i.e., the droplet was in the Cassie-Baxter state. However, on the surfaces with larger intervals between micro-pillars (A03, B03, C03, and D03), the hydrophobic textured surfaces were fully wetted by a water droplet, as shown in Fig. 3(b), i.e., the droplet was in the Wenzel state. On the micro-textured silicon surfaces ( $\theta_0 = 58^\circ$ ), the Wenzel state was observed, as shown in Fig. 4(a). Park *et al.*

reported that droplets on similar silicon surfaces were in a mixed state, where the Wenzel and Cassie state locally co-existed depending on the surface conditions.<sup>16</sup> However, the mixed state was not observed in this study. On the micro-textured surface with MPTS coating ( $\theta_0 = 34^\circ$ ), both the Wenzel and hemi-wicking state were observed depending on the geometric conditions of the surface. On these surfaces, most of the droplets were generally in a Wenzel state. However, on surfaces with a high roughness ratio ( $f_W > 1.5$ ), droplets existed in the precursor (or liquid film) periphery near the contact line, as shown in Fig. 4(b), i.e., the droplets were in the hemi-wicking state.

Subsequently, the experimental results were compared with the model proposed by Bico *et al.*<sup>13</sup> to evaluate the wetting state at the different experimental conditions because their model can be widely applied to the Cassie-Baxter, Wenzel, and hemi-wicking wetting states. In the model of Bico *et al.*, the wetting state of a droplet on a surface is decided based on thermodynamic characteristics; the system of the droplet is favorable in the more stable wetting state under any disturbance. The model estimates the wetting state as follows:

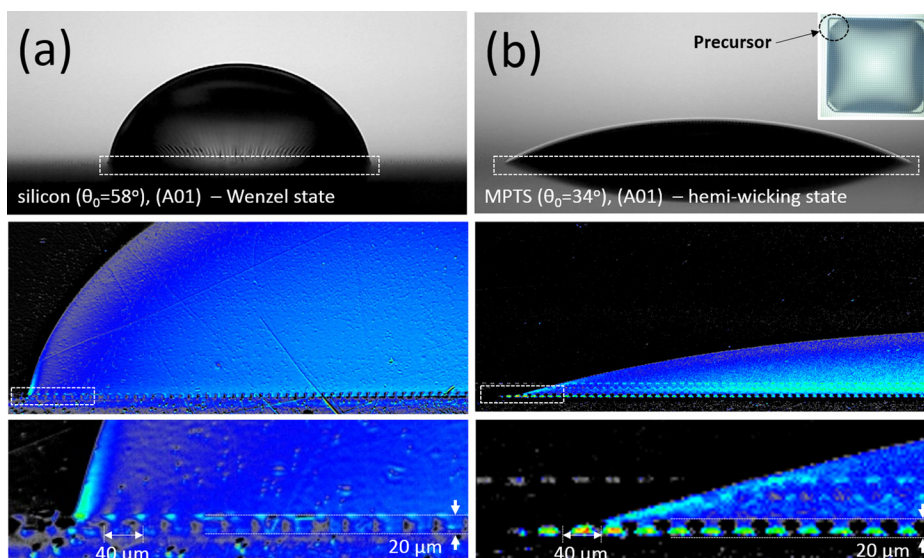


FIG. 4. Visualization of wetting state on micro-textured surfaces using visible light and X-rays (A01:  $d = 15 \mu\text{m}$ ,  $p = 40 \mu\text{m}$ , and  $h = 20 \mu\text{m}$ ); (a) silicon surface and (b) MPTS-coated surface.

$$F_{C-B} = \frac{f_{C-B} - 1}{f_W - f_{C-B}} - \cos \theta_0 \left[ \begin{array}{l} F_{C-B} > 0 \text{ (Cassie-Baxter state)} \\ F_{C-B} < 0 \text{ (Wenzel state)} \end{array} \right], \quad (1)$$

$$F_{hw} = \cos \theta_0 - \frac{1 - f_{C-B}}{f_W - f_{C-B}} \left[ \begin{array}{l} F_{hw} > 0 \text{ (hemi-wicking state)} \\ F_{hw} < 0 \text{ (Wenzel state)} \end{array} \right], \quad (2)$$

where  $F_{C-B}$  and  $F_{hw}$  are the functions used to estimate the wetting state near the Cassie-Baxter and hemi-wicking states, respectively.

However, when the present experimental results were compared with the model of Bico *et al.*, it was found that the model had difficulties in predicting the experimental wetting state under the different surface conditions used. As shown in Fig. 5(a), for the hydrophobic textured surfaces with HDFS coating ( $\theta_0 = 109^\circ$ ), the model of Bico *et al.* estimates that the droplets were only in the Wenzel state within the experimental ranges, although the droplets were mostly in the Cassie-Baxter state, excluding cases A03, B03, C03, and D03. On the textured silicon surfaces ( $\theta_0 = 58^\circ$ ) and the textured silicon surfaces with MPTS coating ( $\theta_0 = 34^\circ$ ), the model estimates that the droplets were in the hemi-wicking state throughout the broad experimental range, as shown in Figs. 5(b) and 5(c), although the droplets were mostly in the Wenzel state (excluding the cases of A01, B01, C01, and D01 on the MPTS-coated surface). Overall, the previous wetting state model estimated that the droplets were in a more wettable state than the experimentally observed wetting state.

In a previous report on wetting phenomena, Kang-Jacobi suggested that energy loss occurs when the contact line of a water droplet is moved. They proposed the following expression for the energy loss in terms of the work of adhesion,  $w$ , based on thermodynamics:<sup>17</sup>

$$\frac{w}{\sigma_{lv}} = \cos \theta_0 + \left( 4 \left( \frac{(2 + \cos \theta_0)(1 - \cos \theta_0)^2}{4} \right)^{2/3} - 2(1 - \cos \theta_0) \right) / \sin^2 \theta_0, \quad (3)$$

where  $\sigma_{lv}$  is the surface tension at the liquid-vapor interface. However, the model of Bico *et al.* neglects the energy loss at the moving contact line when the contact line of the droplet is moved by any disturbance. For good estimation of the wetting state depending on the surface conditions, in this study, we applied the work of adhesion to the model of Bico *et al.* to consider the energy loss at the moving contact line under any distribution. Assuming isothermal and isochoric conditions for a small displacement under any disturbance, the system of a droplet on the surface can be defined with the Helmholtz free energy,  $H$ . To determine the wetting state of such a droplet on both hydrophilic and hydrophobic textured surfaces, Eqs. (4) and (5) were derived to define the relationship between wetting states based on the consideration that the system of a droplet on the surface is favorable in the more stable wetting state under any disturbance. Therefore,

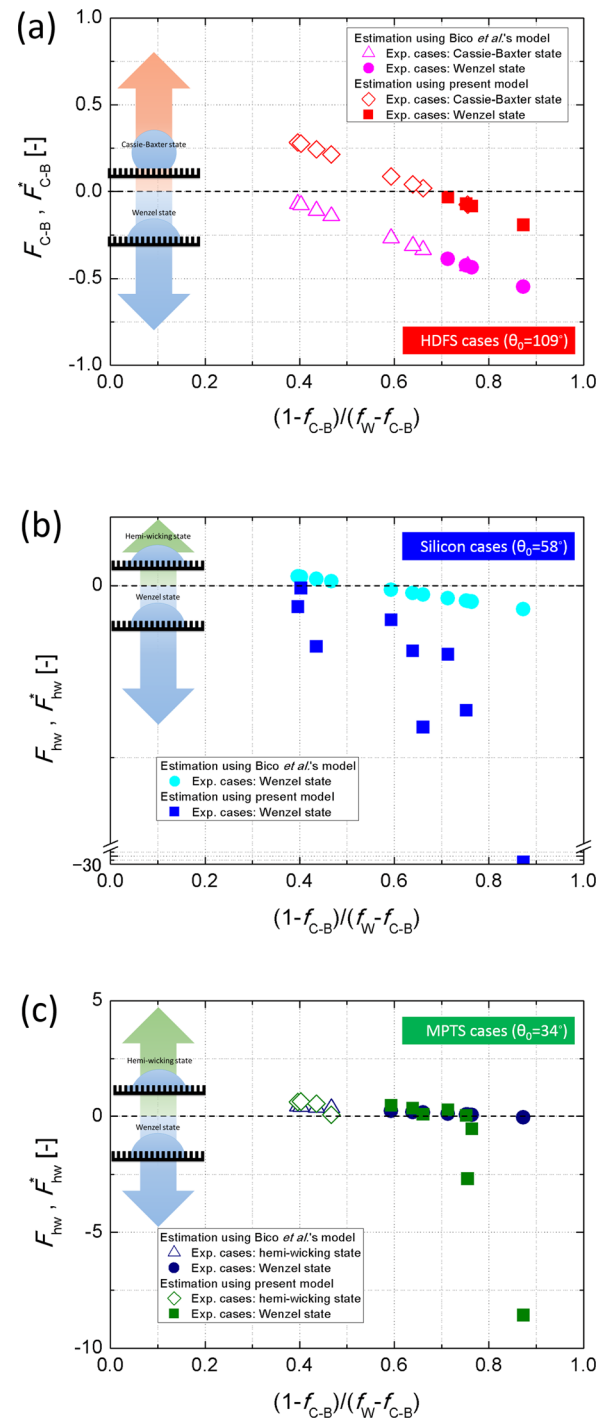


FIG. 5. Estimation of wetting state by the model of Bico *et al.*<sup>13</sup> and presently developed model. (a) Experimental data for HDFS-coated textured surfaces. (b) Experimental data for silicon textured surfaces. (c) Experimental data for MPTS-coated textured surfaces.

the developed thermodynamic model for estimating the wetting state is

$$\frac{dH_{C-B}}{dL} < \frac{dH_W}{dL}; \text{ Cassie-Baxter state is favorable}$$

$$F_{C-B}^* = \frac{f_{C-B} - 1}{f_W - f_{C-B}} + \frac{w}{\sigma_{lv}} - \cos \theta_0 \left[ \begin{array}{l} F_{C-B}^* > 0 \text{ (Cassie-Baxter state)} \\ F_{C-B}^* < 0 \text{ (Wenzel state)} \end{array} \right], \quad (4)$$

$$\frac{dH_{hw}}{dL} < \frac{dH_W}{dL}; \text{ hemi-wicking state is favorable}$$

$$F_{hw}^* = 1 + \frac{\cos \theta_A - 1}{f_{C-B}} + \frac{w}{\sigma_{lv}}$$

$$- \cos \theta_0 \left[ \begin{array}{l} F_{hw}^* > 0 \text{ (hemi-wicking state)} \\ F_{hw}^* > 0 \text{ (Wenzel state)} \end{array} \right], \quad (5)$$

where  $F_{C-B}^*$  and  $F_{hw}^*$  are the modified functions used to estimate the wetting state about the Cassie-Baxter state and hemi-wicking state, respectively. Additionally, the apparent contact angle  $\theta_A$  was estimated with the Kang-Jacobi wetting model to consider the energy loss during movement of the contact line of the water droplet, as shown in Eq. (6)

$$1 - \cos \theta_A - 2 \frac{\left[ \frac{(2 + \cos \theta_A)(1 - \cos \theta_A)^2}{4} \right]^{2/3}}{\sin^2 \theta_A}$$

$$= f_W \frac{1 - \cos \theta_0 - 2 \left[ \frac{(2 + \cos \theta_0)(1 - \cos \theta_0)^2}{4} \right]^{2/3}}{\sin^2 \theta_0}. \quad (6)$$

The detailed derivation of Eqs. (4) and (5) is described in the supplementary material.<sup>38</sup>

The developed model for estimating the wetting state was first tested with the experimental results obtained for the textured surfaces with HDFs coating ( $\theta_0 = 109^\circ$ ), as shown in Fig. 5(a). The experimental data were well estimated by the developed model, excluding case A02. On the textured silicon surfaces ( $\theta_0 = 58^\circ$ ), the experimental data were well estimated by the developed model within the experimental ranges, as shown in Fig. 5(b). On the textured surfaces with MPTS coating ( $\theta_0 = 34^\circ$ ), however, the developed model poorly estimated the wetting state because it predicted a hemi-wicking state across the experimental ranges, similar to the predictions by the previous model. However, as shown in Fig. 5(c), it is noted that the present model provided a more accurate fit to the experimental results than that by the previous model.

For cases A02 of the HDFs-coated surfaces, and B02, C02, C03, D02, and D03 of the MPTS-coated surfaces, the poor prediction of the present model originated from potential surface defects generated during the fabrication stage. When the micro-textured surface was fabricated with deep reactive ion etching, scallop shapes at the sidewall of the micro-pillars were generated, as shown in Fig. 2(b). According to the previous reports,<sup>39</sup> discontinuities on a surface increase the total system energy owing to frictional resistance on the contact line when displacement along the contact line occurs by a purely mechanical process. Therefore, the poor estimation of these cases using the developed model occurred because their wetting states were metastable (not stable). In future work, the energy or friction resistance at the scallop shape of the micro-pillars should be researched quantitatively to allow their effects to be overcome.

In summary, we investigated wetting states on hydrophilic and hydrophobic micro-textured surfaces. The dependence of wetting state on the surface conditions of well-quantified micro-textured surfaces was clearly visualized using synchrotron X-ray radiography. When the

experimental results were compared with the previous wetting state model of Bico *et al.*, the model estimated that the droplets had a more wettable state than the experimentally observed wetting state. Therefore, we developed a thermodynamic model to take energy loss that occurred during movement of the contact line into consideration. It was found that our model well estimated the wetting state when the energy loss at the moving contact line was considered.

This work was supported by the National Research Foundation of Korea (NRF) Grants funded by the Korean Government (MSIP) (2014M2B2A9031122). Experiments at the Pohang Light Sources were supported in part by MSIP and POSTECH.

- <sup>1</sup>R. N. Wenzel, *Ind. Eng. Chem.* **28**(8), 988 (1936).
- <sup>2</sup>R. N. Wenzel, *J. Phys. Chem.* **53**(9), 1466 (1949).
- <sup>3</sup>A. Nakajima, K. Hashimoto, T. Watanabe, K. Taki, G. Yamaguchi, and A. Fujishima, *Langmuir* **16**(17), 7044 (2000).
- <sup>4</sup>R. Fürstner, W. Barthlott, C. Neinhuis, and P. Walzel, *Langmuir* **21**(3), 956 (2005).
- <sup>5</sup>H. Höcker, *Pure Appl. Chem.* **74**(3), 423 (2002).
- <sup>6</sup>C.-H. Choi and C.-J. Kim, *Phys. Rev. Lett.* **96**, 066001 (2006).
- <sup>7</sup>A. Marmur, *Langmuir* **22**(4), 1400 (2005).
- <sup>8</sup>J. Genzer and A. Marmur, *MRS Bull.* **33**(8), 742 (2008).
- <sup>9</sup>J. B. Boreyko and C.-H. Chen, *Phys. Rev. Lett.* **103**, 184501 (2009).
- <sup>10</sup>H. S. Ahn, H. J. Jo, S. H. Kang, and M. H. Kim, *Appl. Phys. Lett.* **98**(7), 071908 (2011).
- <sup>11</sup>K.-H. Chu, R. Enright, and E. N. Wang, *Appl. Phys. Lett.* **100**(24), 241603 (2012).
- <sup>12</sup>K.-H. Chu, Y. S. Joung, R. Enright, C. R. Buie, and E. N. Wang, *Appl. Phys. Lett.* **102**(15), 151602 (2013).
- <sup>13</sup>J. Bico, U. Thiele, and D. Quéré, *Colloids Surf., A* **206**(1–3), 41 (2002).
- <sup>14</sup>C. Ishino and K. Okumura, *Eur. Phys. J. E* **25**(4), 415 (2008).
- <sup>15</sup>A. Cassie and S. Baxter, *Trans. Faraday Soc.* **40**, 546 (1944).
- <sup>16</sup>C. I. Park, H. E. Jeong, S. H. Lee, H. Y. Cho, and K. Y. Suh, *J. Colloid Interface Sci.* **336**(1), 298 (2009).
- <sup>17</sup>H. C. Kang and A. M. Jacobi, *Langmuir* **27**(24), 14910 (2011).
- <sup>18</sup>A. Lafuma and D. Quéré, *Nat. Mater.* **2**, 457 (2003).
- <sup>19</sup>D. Quéré, A. Lafuma, and J. Bico, *Nanotechnology* **14**, 1109 (2003).
- <sup>20</sup>N. A. Patankar, *Langmuir* **20**(17), 7097 (2004).
- <sup>21</sup>C. Ishino, K. Okumura, and D. Quéré, *Europhys. Lett.* **68**(3), 419 (2004).
- <sup>22</sup>C. Ishino and K. Okumura, *Europhys. Lett.* **76**(3), 464 (2006).
- <sup>23</sup>S. Moulinet and D. Bartolo, *Eur. Phys. J. E* **24**, 251 (2007).
- <sup>24</sup>Y. C. Jung and B. Bhushan, *Scr. Mater.* **57**(12), 1057 (2007).
- <sup>25</sup>B. Bharat, M. Nosonovsky, and Y. C. Jung, *J. R. Soc., Interfaces* **4**(15), 643 (2007).
- <sup>26</sup>M. Sbragaglia, A. M. Peters, and C. Pirat, *Phys. Rev. Lett.* **99**, 156001 (2007).
- <sup>27</sup>M. Reyssat, J. M. Yeomans, and D. Quéré, *Europhys. Lett.* **81**(2), 26006 (2008).
- <sup>28</sup>K.-Y. Yeh and L.-J. Chen, *Langmuir* **24**(1), 245 (2008).
- <sup>29</sup>P. Tsai, R. G. H. Lammertink, M. Wessling, and D. Lohse, *Phys. Rev. Lett.* **104**, 116102 (2010).
- <sup>30</sup>P. Forsberg, F. Nikolajeff, and M. Karlsson, *Soft Matter* **7**(1), 104 (2011).
- <sup>31</sup>N. A. Patankar, *Langmuir* **26**(11), 8941 (2010).
- <sup>32</sup>H.-M. Kwon, A. T. Paxson, K. K. Varanasi, and N. A. Patankar, *Phys. Rev. Lett.* **106**, 036102 (2011).
- <sup>33</sup>E. Bormashenko, A. Musin, G. Whyman, and M. Zinigrad, *Langmuir* **28**(7), 3460 (2012).
- <sup>34</sup>A. Giacomello, S. Meloni, M. Chinappi, and C. M. Casciola, *Langmuir* **28**(29), 10764 (2012).
- <sup>35</sup>P. Papadopoulos, L. Mammen, X. Deng, D. Vollmer, and H.-J. Butt, *Proc. Natl. Acad. Sci. U.S.A.* **110**(9), 3254 (2013).
- <sup>36</sup>R. David and A. W. Neumann, *Colloids Surf., A* **425**, 51 (2013).
- <sup>37</sup>D. Murakami, H. Jinnai, and A. Takahara, *Langmuir* **30**(8), 2061 (2014).
- <sup>38</sup>See supplementary material at <http://dx.doi.org/10.1063/1.4919136> for the definition of the roughness ratio, specific visualization procedure using synchrotron X-ray radiography, the derivation of the thermodynamic model, and tables for Fig. 5.
- <sup>39</sup>J. W. Gibbs, *Scientific Report of J. Willard Gibbs: Thermodynamics* (Green and Company, London, 1906).